

Sensors

A 1,3-Capped Calix[4] Conjugate Possessing an Amine Moiety as an Anion Receptor: Reversible Anion Sensing Detected by Spectroscopy and Characterization of the Supramolecular Features by Microscopy

Anita Nehra, Deepthi S. Yarramala, and Chebrolu Pulla Rao*^[a]

Abstract: A phenylenediamine-capped conjugate of calix[4]-arene (L_{amino}) was synthesized by reducing its precursor, L_{imino} with sodium borohydride in methanol. The L_{amino} sample binds to anions due to the more flexible and bent conformation of the capped aminophenolic binding core, compared to the precursor L_{imino} . The L_{amino} sample showed selectivity towards $H_2PO_4^-$ by exhibiting a ratiometric increase in emission by about 11-fold with a detection limit of $(1.2 \pm 0.2) \mu\text{M}$ ((116 ± 20) ppb) over 15 anions studied, including other phosphates, such as $P_2O_7^{4-}$, adenosine monophosphate (AMP^{2-}), adenosine diphosphate (ADP^{2-}), and adenosine triphosphate (ATP^{2-}). The L_{amino} sample shows an increase in the absorbance at $\lambda = 315$ nm in the presence of $H_2PO_4^-$, CO_3^{2-} , HCO_3^- , $CH_3CO_2^-$, and F^- . The 1H NMR spectroscopic titration of L_{amino} with $H_2PO_4^-$, F^- , and $CH_3CO_2^-$ showed major changes in the phenylene-capped and salicyl

moieties, and thereby, confirming the aminophenolic region as the binding core. However, the binding strength of these anions followed the trend $H_2PO_4^- > F^- \gg CH_3CO_2^- > HSO_4^-$. The heat changes observed by isothermal titration calorimetry support this trend. The L_{amino} sample showed reversible sensing towards $H_2PO_4^-$ and F^- in the presence of Mg^{2+} and Ca^{2+} , respectively. NOESY studies of L_{amino} in comparison with its anionic complexes, revealed that major conformational changes occurred in the capping region to facilitate the binding of anion. ESI-MS and the Job's method revealed 1:1 stoichiometry between L_{amino} and $H_2PO_4^-$ or F^- . In the SEM micrographs of L_{amino} the spherical particles are converted into spherical aggregates and further form large agglomerates and even branched sheets in the presence of anions, depending upon their binding strength.

Introduction

The synthesis of a novel receptor possessing an inherent capability to modify its photophysical properties upon interaction with anions is of great interest to chemists because such a receptor can act as a sensor.^[1–13] Anion sensing by typical supramolecular scaffolds, such as calixpyrrole,^[14–17] azacyclophanes,^[18] calixarenes,^[19–21] and cucurbiturils,^[22] has been documented in the recent literature. Among these systems, calixarenes were preferential owing to the ease of functionalization on both the upper and lower rims, and the presence of a preorganized core, which is required to improve ion selectivity.^[23–26] Calix[*n*]arenes possessing urea/thiourea^[27] and amide^[28,29] moieties were developed as anion sensors in which the interactions were mainly manifested by hydrogen bonding and were

electrostatic when a quaternized ammonium center^[30] was present. In addition, the metal-ion complexes of calix conjugates have been developed as anion sensors.^[31,32] However, calix[4]arene conjugates that possess a reduced imine moiety ($-H_2C-NH-$) and exhibit selective recognition for phosphates and such systems are rather scarce in the literature.

Phosphates play crucial roles in biology wherein $H_2PO_4^-$ is involved in a variety of biological processes.^[33–39] Therefore, the detection of $H_2PO_4^-$ selectively among other biologically relevant phosphates, such as adenosine monophosphate (AMP^{2-}), adenosine diphosphate (ADP^{2-}), and adenosine triphosphate (ATP^{2-}), is very important.^[40–53] Recently, we reported an anthracenyl-appended triazole-linked receptor that was selective to Co^{2+} .^[54] When this receptor was quaternized at the triazole nitrogen atoms, effective binding to biologically relevant triphosphates was obtained.^[55] Therefore, herein, we report a phenylenediamine-capped conjugate of calix[4]arene, 5,11,17,23-*tert*-butyl-25,27-bis-([phenylenebis(azanediyl)]-bis(methylene)-bis(*tert*-butyl-2-methyl)phenoltriazolylmethoxy)-26,28-dihydroxycalix[4]arene (L_{amino}), that results in the loss of Mg^{2+} cation sensing^[56] and further transforms into a molecular system that selectively senses anionic $H_2PO_4^-$ through a ratiometric fluorescence response. The binding strengths of anions were assessed by isothermal titration calorimetry (ITC). Such anion sensing

[a] Dr. A. Nehra, D. S. Yarramala, Prof. C. P. Rao
Bioinorganic Laboratory, Department of Chemistry
Indian Institute of Technology Bombay, Powai
Mumbai 400076 (India)
Fax: (+91) 22-2572-3480
E-mail: cp Rao@iitb.ac.in

Supporting information for this article is available on the WWW under
<http://dx.doi.org/10.1002/chem.201600609>.

can also be identified based on changes that occur in supra-molecular aggregations of the receptor, as observed by SEM.

Experimental Section

Absorption and fluorescence studies

Bulk solutions of L_{amino} and the salts (possessing the requisite anion) were prepared in acetonitrile at a concentration of 6×10^{-4} M. Bu_4N^+ salts were used in case of F^- , Cl^- , Br^- , I^- , $H_2PO_4^-$, CO_3^{2-} , ClO_4^- , HSO_4^- , and $CH_3CO_2^-$; Na^+ salts were used in case of HCO_3^- , NO_3^- , SO_4^{2-} , $P_2O_7^{4-}$, AMP^{2-} , ADP^{2-} , and ATP^{2-} anions. All fluorescence titrations were carried out at $\lambda_{\text{ex}} = 290$ nm. Excitation and emission slit widths used were 5 nm and a scan speed of 200 nm min^{-1} was used. Absorption studies were carried out on a JASCO V-570 spectrometer. All fluorescence and absorption titrations were carried out in 1 cm quartz cells by maintaining a final $[L_{\text{amino}}]$ of $5 \mu\text{M}$ in a total volume of 3 mL; this was achieved by diluting with acetonitrile.

^1H NMR spectroscopy studies

^1H NMR spectroscopy studies were carried out in CDCl_3 at 25°C at 400 MHz on a Bruker NMR spectrometer. Bu_4N^+ salts were used for all anions used in this study. Solutions (40 mM) of the corresponding anion were gradually added to a 4 mM solution of L_{amino} (0.5 mL) during the titrations. 2D NMR studies were performed in CDCl_3 ; $[L_{\text{amino}}] = 5 \text{ mM}$.

Isothermal titration calorimetry (ITC)

The calorimetric titrations were performed at 20°C with a MicroCal ITC 200 isothermal titration calorimeter from MicroCal (Northampton, MA, USA). The corresponding anion, as a 0.5 mM solution (40 μL) in a syringe, was added to a 0.1 mM solution of ligand L_{amino} in the cell by means of 20 injections. The first addition was 0.2 μL and successive additions of 2 μL were given by maintaining a time spacing of 150 s between each injection. The ITC data were fitted with the origin software package provided by MicroCal by using one set of site curve-fitting models. Each time a control was carried out without L_{amino} and the corresponding data were subtracted from the main titration data; the resultant data was subjected to the curve-fitting procedure.

Sample preparation for SEM

For SEM studies, aliquots (40 μL) of L_{amino} (5 μM) and L_{amino} + anions in acetonitrile were sonicated for 15–20 min and the samples were drop-cast on an aluminum surface and dried under an IR lamp.

Synthesis and characterization of L_{amino}

Synthesis and characterization of all precursors were the same as that reported recently.^[56] The L_{imino} derivative (0.1 g, 0.08 mmol) was taken in dry methanol (5 mL) before NaBH_4 (0.06 g, 0.0016 mol) was added at 0°C and the mixture was stirred for 1 h at room temperature. The solvent was evaporated under vacuum, water (10 mL) was added to the residue, and the product was extracted into dichloromethane ($3 \times 10 \text{ mL}$). The collected organic layer was washed with water ($2 \times 10 \text{ mL}$), followed by brine, and was dried over anhydrous Na_2SO_4 . Removal of the solvent under reduced pressure afforded L_{amino} as a pure product (0.05 g, 50%). ^1H NMR (CDCl_3): $\delta = 8.14$ (s, 2H; triazole-H), 7.29 (d; Ar-H), 7.10 (d; Ar-H), 6.98 (s, 2H; calix-Ar-H), 6.89 (s, 2H; Ar-H), 6.87 (s, 2H; Ar-H),

6.82 (s, 4H; Ar-OH), 6.68 (s, 2H; Ar-H), 5.5 (s, 4H; Sal- CH_2), 5.1 (s, 4H; Ar- OCH_2), 4.27 (s, 4H; Ar- CH_2 -Ar), 4.13 (d, 4H; Ar- CH_2 -Ar), 3.1 (d, 4H; Ar- CH_2 -Ar), 1.29 & 1.27 (d, 18H, $-\text{C}(\text{CH}_3)_3$), 0.90 ppm (s, 18H; Ar- $(\text{CH}_3)_3$); ^{13}C NMR (CDCl_3): $\delta = 153.6$, 151.2, 150.8, 147.8, 144.6, 143.8, 142.5, 137.5, 132.9, 128.8, 127.7, 127.6, 126.3, 125.7, 125.1, 123.9, 122.3, 115.8, 70.0, 50.1, 48.9, 34.3, 34.07, 34.04, 31.9, 31.8, 31.7, 31.6, 31.1 ppm; HRMS: m/z calcd for $\text{C}_{80}\text{H}_{95}\text{O}_6\text{N}_8$ $[M+1]^+$: 1267.7688; found: 1267.7738; elemental analysis calcd (%) for $\text{C}_{82}\text{H}_{106}\text{N}_8\text{O}_8$ ($L + 2\text{CH}_3\text{OH}$): C 73.95, H 8.02, N 8.41; found: C 73.62, H 6.74, N 8.19.

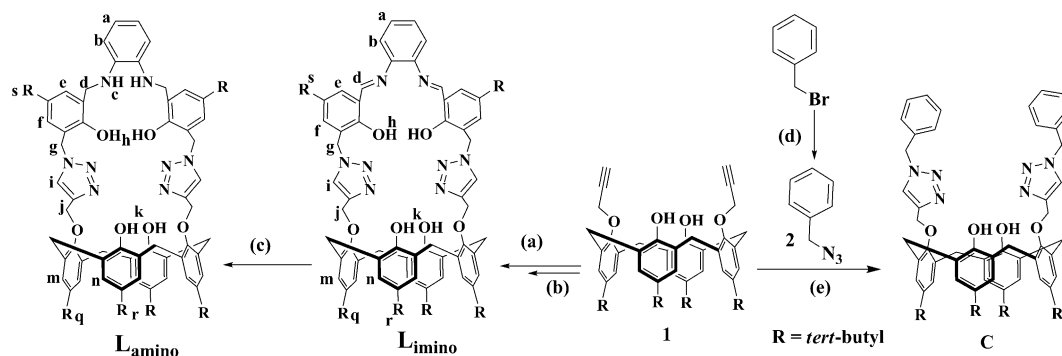
Synthesis and characterization of C

Compound 1 (0.1 g, 0.08 mmol) and benzyl azide (2; 0.15 g, 1.18 mmol) were dissolved in a mixture of dichloromethane, *tert*-butanol, and water (20 mL, 1:1:2). $\text{CuSO}_4 \cdot 5\text{H}_2\text{O}$ (0.03 g, 1.15 mmol) and sodium ascorbate (0.05 g, 0.23 mmol) were then added. The resulting solution was stirred for 12 h at room temperature. Upon completion of the reaction (based on TLC), the organic layer was separated and the aqueous layer was extracted with dichloromethane ($2 \times 50 \text{ mL}$). The combined organic layer was washed with brine ($2 \times 50 \text{ mL}$), dried over Na_2SO_4 , the solvent was removed under reduced pressure, and hexane was added to give C as a pure white product (0.09 g, 64%). ^1H NMR (CDCl_3 , 400 MHz): $\delta = 0.96$ (s, 18H; $\text{C}(\text{CH}_3)_3$), 1.27 (s, 18H; $\text{C}(\text{CH}_3)_3$), 3.19 (d, $J = 15.08 \text{ Hz}$, 4H; Ar- $\text{CH}_{2\text{eq}}$ -Ar), 4.12 (d, $J = 15.24 \text{ Hz}$, 4H; Ar- $\text{CH}_{2\text{ax}}$ -Ar), 5.1 (s, 4H; Ar- CH_2), 5.54 (s, 4H; OCH_2), 6.7 (s, 4H; Ar-H), 6.9 (s, 4H; Ar-H), 7.2 (s, 2H; Ar-OH), 7.26 (m, 4H; Ar-H), 7.34 (m, 6H; Ar-H), 7.82 ppm (s, 2H; triazole-H); ^{13}C NMR (CDCl_3 , 100 MHz): $\delta = 31.2$, (Ar- CH_2 -Ar), 31.9, 32.0, 34.0, 34.2, 54.4, 66.7 ($-\text{O}-\text{CH}_2$), 123.8, 125.3, 125.9, 127.9, 128.3, 128.8, 129.2, 132.9, 135.2, 141.9, 144.6, 147.5, 149.7, 150.6 ppm; ESI-MS: m/z : 991 $[M+1]$.

Results and Discussion

The phenylenediamine-appended, triazole-linked calix[4]arene L_{amino} was synthesized in a single step from L_{imino} by the reduction of the imine group with NaBH_4 , as described in the Experimental Section (Scheme 1). The L_{amino} sample was characterized by ^1H and ^{13}C NMR, COSY, and NOESY spectroscopy, ESI-MS, and elemental analysis (SI 01 in the Supporting Information).

The conjugate L_{amino} exists in a cone conformation in solution, as evident from the ^1H NMR spectrum, which exhibits two doublets at $\delta = 3.10$ and 4.13 ppm that correspond to the bridge CH_2 groups of the calixarene rim. As the electronic environment in the capped arm region changes upon reduction, the chemical shifts of protons e and f were affected considerably due to the conversion of $-\text{HC}=\text{N}-$ (L_{imino}) into $-\text{H}_2\text{C}-\text{NH}-$ (L_{amino}). As a result of the conversion of imine to amine, the $\Delta\delta_{\text{e,f}}$ value changes from 0.34 to 0.01 ppm; the environments of e and f turn out to be identical. Signals a and b were identified at $\delta = 7.29$ and 7.21 ppm, respectively, by COSY due to cross correlations (Figure 1 a). Conformational changes that occurred in the capped arms upon reduction of the imine moiety were supported by NOESY results (Figure 1 b). The set of protons a and g show strong correlations in the NOESY spectrum, which suggest that the capped region is bent to a large extent due to the presence of $-\text{H}_2\text{C}-\text{NH}-$ (L_{amino}), thereby introducing greater flexibility than that of $-\text{HC}=\text{N}-$ present in L_{imino} . This is



Scheme 1. Synthesis of **L_{amino}** and **C**: a) 3-(azidomethyl)-5-*tert*-butyl-2-hydroxybenzaldehyde, CuSO₄·5H₂O, sodium ascorbate, dichloromethane/water (1:1), RT, 12 h (≈ 90%); b) *o*-phenylenediamine, CH₃OH, RT, 12 h (74%); c) NaBH₄, CH₃OH, RT, 1 h; d) NaN₃, DMSO, RT, 12 h; e) **2**, CuSO₄·5H₂O, sodium ascorbate, *t*BuOH/water (1:1), RT, 12 h.

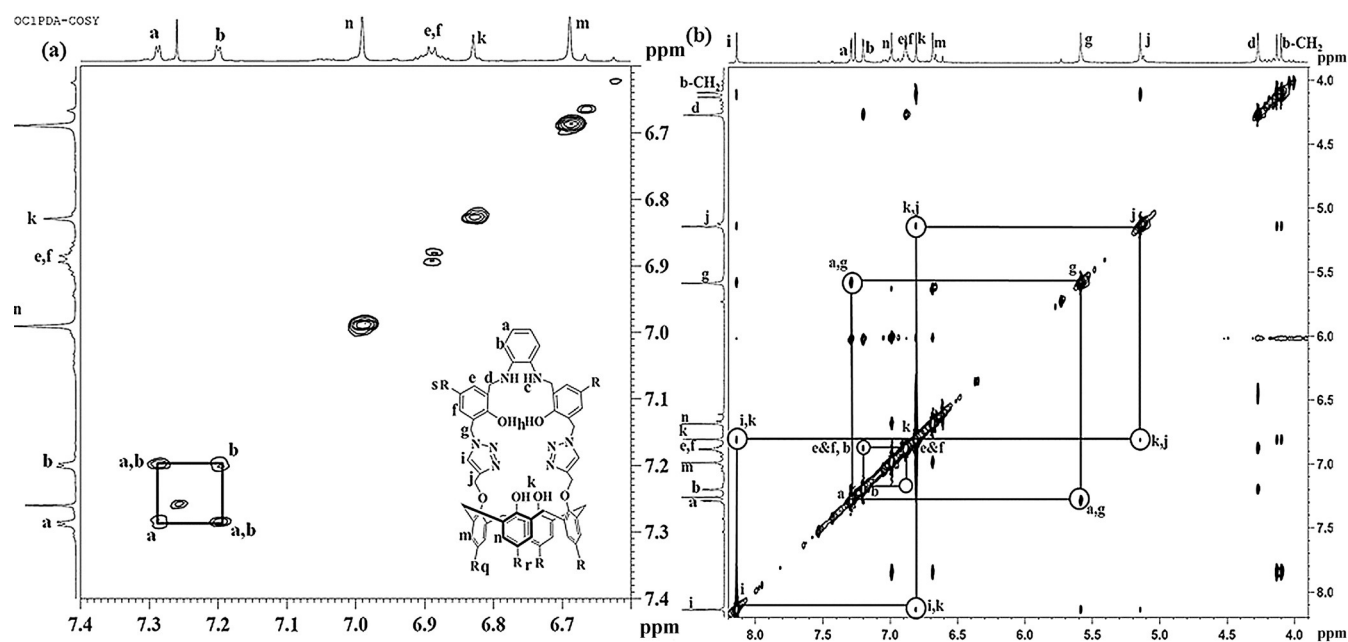


Figure 1. Two-dimensional ¹H NMR spectra of **L_{amino}**: a) COSY, b) NOESY.

further supported by a weak correlation observed between b and e and f. The calix[4]arene conformation is still a cone in the case of **L_{amino}**.

The **L_{amino}** sample has been subjected to anion-binding studies by ¹H NMR, absorption, and fluorescence spectroscopy, and the masses of the species were established by ESI-MS. The control, **C**, was synthesized from **2** and dipropargyl (**1**) through a click reaction and was characterized (SI 02 in the Supporting Information). Control **C** was used to affirm the necessity of the capped aminophenolic binding core for receiving the anion.

Response towards anions

The interactions of **L_{amino}** with anions have been studied by ESI-MS and ¹H NMR, fluorescence, and absorption spectroscopy.

Absorption studies

The binding of anions to **L_{amino}** has been evaluated by carrying out absorption titrations with different anions, such as halides (F⁻, Cl⁻, Br⁻, I⁻), phosphates (H₂PO₄⁻, P₂O₇⁴⁻, AMP²⁻, ADP²⁻, and ATP²⁻), and other oxoanions (CO₃²⁻, NO₃⁻, SO₄²⁻, ClO₄⁻, HSO₄⁻, HCO₃⁻, CH₃CO₂⁻), in acetonitrile. The **L_{amino}** sample exhibited an absorption band centered at λ = 290 nm that corresponded to π-π* transitions (Figure 2a). Upon titration, some of these anions exhibited a new band at λ = 315–320 nm (Figure 2a), the absorbance of which increased with increasing concentration of the added anion. This new band is attributable to intermolecular charge transfer (ICT) between the anion and NH of **L_{amino}**, through which the interaction leads to hydrogen bonding. Considerable changes of this type were observed with F⁻, among the halides; with H₂PO₄⁻, among the phosphates; and with HCO₃⁻, CO₃²⁻, and CH₃CO₂⁻, among the

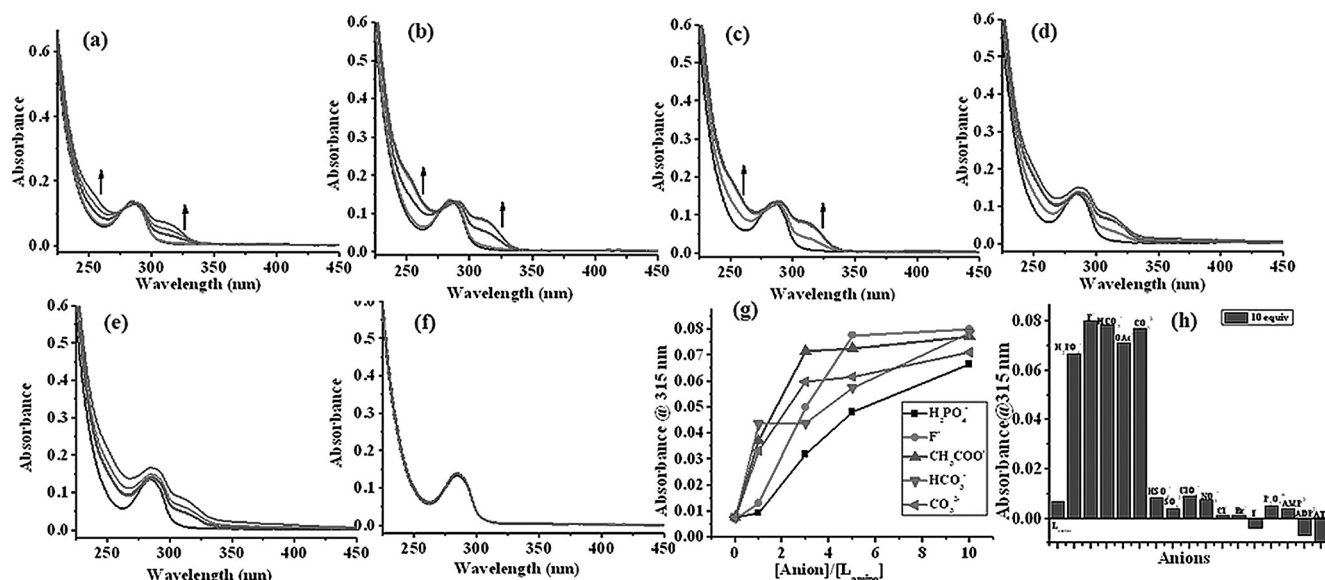


Figure 2. Absorption spectra obtained during the titration of L_{amino} with anions: a) H_2PO_4^- , b) F^- , c) CH_3CO_2^- , d) CO_3^{2-} , e) HCO_3^- , and f) HSO_4^- . g) Absorbance versus molar ratio plots for all anion titrations. h) Histogram showing changes in the absorbance of L_{amino} at $\lambda = 315$ nm in the presence of anions.

other oxoanions studied (Figure 2 b–f and SI 03 in the Supporting Information). The changes observed in absorbance in the new band were plotted as a function of the molar ratio of the anion added for all five anions (Figure 2g). An increase in the absorbance of $\lambda \approx 255$ –260 nm was observed for all five anions (Figure 2a–e). The other 11 anions studied showed no considerable change to the absorption spectra; Figure 2f shows the spectra for one such case: HSO_4^- . The highest absorbance observed in the new band is shown as a histogram in Figure 2h, from which the five strongly interacting and binding ions can be easily identified. To understand the relative interaction abilities of these five anions with L_{amino} , further studies were carried out by fluorescence and ^1H NMR spectroscopy.

Fluorescence studies

The L_{amino} sample exhibited an emission band at $\lambda = 315$ nm upon excitation at $\lambda = 290$ nm in acetonitrile, and was titrated with each of those anions listed for the absorption studies (SI 04 in the Supporting Information). When L_{amino} is titrated against H_2PO_4^- , it shows a decrease in the fluorescence intensity of the band at $\lambda = 315$ nm and a concomitant increase in a new emission band at $\lambda = 425$ nm, with a clear isoemissive point at $\lambda = 372$ nm (Figure 3a and b). Thus, the L_{amino} sample exhibited a ratiometric response towards the incremental addition of H_2PO_4^- , which implied the interaction of the conjugate with the anion. Emission is attributed to the presence of hydrogen-bonding interactions and to the aggregational behavior of the complexes with anions. Such blue emission has been reported in the literature.^[57] The quantum yield of L_{amino} is 0.0024, which is enhanced by about 10-fold in the presence of H_2PO_4^- , and is 0.026 with respect to 2-aminopyridine (SI 05 in the Supporting Information). The 1:1 stoichiometry between L_{amino} and H_2PO_4^- was established based on the Job method

(SI 06 in the Supporting Information). The binding constant derived based on this data by using the Benesi–Hildebrand equation resulted in $K_a = 6.18 \times 10^4 \text{ M}^{-1}$ for the binding of H_2PO_4^- by L_{amino} (SI 07 in the Supporting Information). The minimum detection limit observed is $(1.2 \pm 0.2) \mu\text{M}$ ((116 ± 20) ppb; SI 08 in the Supporting Information). To investigate the effect of H_2O , a similar titration was performed in a 5% aqueous solution of CH_3CN (v/v), in which L_{amino} exhibited a 3- to 4-fold increase in fluorescence intensity at $\lambda = 425$ nm when H_2PO_4^- was added (SI 04 in the Supporting Information). No other phosphate ion, namely, $\text{P}_2\text{O}_7^{4-}$, AMP^{2-} , ADP^{2-} , and ATP^{2-} , studied showed any change in the fluorescence emission of L_{amino} .

Similar fluorescence studies carried out with the halides resulted in a ratiometric change only in case of F^- and not with other halides; however, the extent to which the $\lambda \approx 430$ nm band increased was much lower in case of F^- than that of H_2PO_4^- . Of all other oxoanions studied, only CH_3CO_2^- , CO_3^{2-} , and HCO_3^- exhibited similar ratiometric changes, although the increase in intensity observed for the $\lambda \approx 430$ nm band was much lower and comparable to that observed with F^- . Based on the ratiometric enhancement of I_{425}/I_{315} , the anion interacting ability follows the order $\text{H}_2\text{PO}_4^- \gg \text{F}^- \approx \text{CO}_3^{2-} \approx \text{CH}_3\text{CO}_2^- \geq \text{HCO}_3^-$ (Figure 3b–f). This enhancement is at least four- to six-fold higher for H_2PO_4^- than that of any other anion, which suggests that the interaction with this ion is stronger and may result in greater changes to the conformation of the arms. The relative fluorescence intensity pertaining to the $\lambda = 420$ nm band is shown in Figure 3g as a histogram for all anions. No other anions showed significant changes in the fluorescence spectra of L_{amino} and were the same as that of HSO_4^- given in Figure 3h.

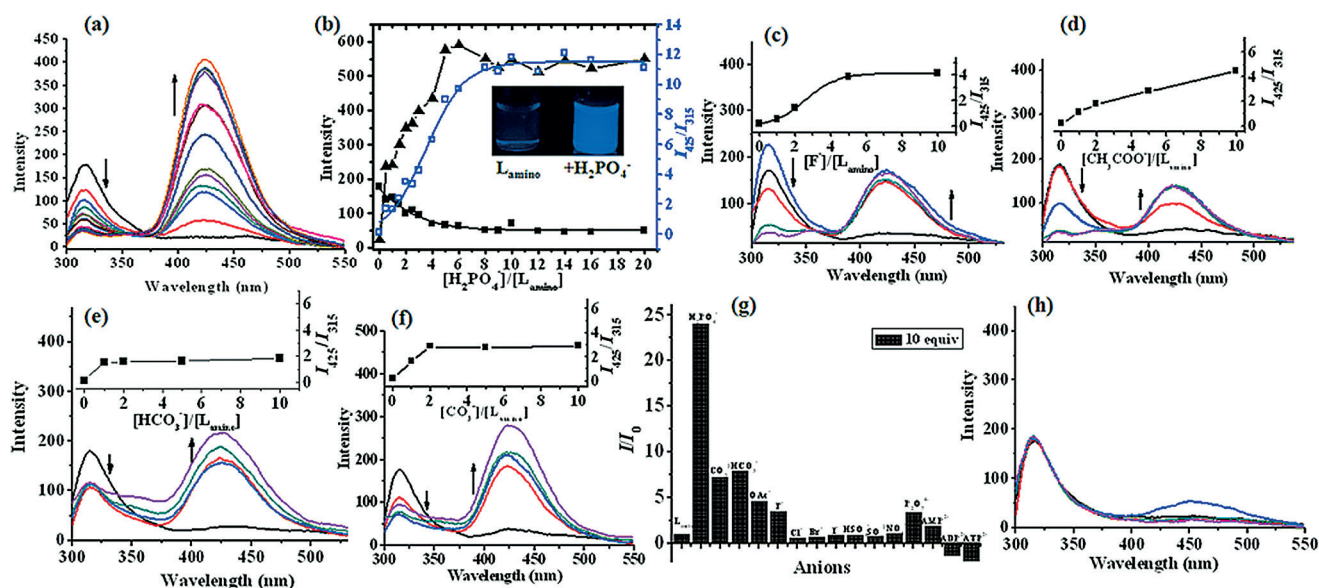


Figure 3. Fluorescence spectra obtained during the titration of L_{amino} with anions: a) $H_2PO_4^-$, c) F^- , d) $CH_3CO_2^-$, e) HCO_3^- , f) CO_3^{2-} , and h) HSO_4^- . b) The titration of L_{amino} with $H_2PO_4^-$ is shown as molar ratio versus intensity (squares: $\lambda = 315$ nm, triangles: $\lambda = 425$ nm); the blue line indicates the molar ratio versus ratiometric response. Inset: photographs of vials under a UV lamp. g) Histogram showing the relative intensity for the band at $\lambda = 425$ nm with 10 equivalents of anions.

1D and 2D NMR spectroscopy studies with anions

Having observed that $H_2PO_4^-$, F^- , and $CH_3CO_2^-$ ions showed considerable changes in their absorption and emission spectra, we carried out 1H NMR spectral studies with these ions (SI 09 in the Supporting Information). In addition, another ion that did not show any change in absorption and emission, namely, HSO_4^- was also studied by 1H NMR spectroscopy to further prove that this ion indeed did not bind to L_{amino} (SI 09 in the Supporting Information). When $H_2PO_4^-$ is added to L_{amino} incrementally, signals corresponding to the phenylene motif (a, b) and salicyl moiety (e, f, s) shift upfield, whereas the signal observed at $\delta = 4.2$ ppm (d) undergoes a downfield shift, which supports the hypothesis that $H_2PO_4^-$ interacts with L_{amino} in this region. However, the signal of the triazole proton (i) and calixarene platform signals (m, n, q, r) exhibit negligible changes upon the addition of $H_2PO_4^-$ (Figure 4).

The following are some important comparisons observed from the 1H NMR spectra upon titration with different anions. 1) The triazole proton i exhibits a large downfield shift by about 0.22 ppm ($\Delta\delta$) only in presence of F^- ; the other anions showed negligible changes (Figure 4b and c). 2) The $-CH_2$ (d) signal shifted downfield by about 0.12 ppm in the presence of $H_2PO_4^-$, whereas in the case of F^- the signal shifted upfield by about 0.1 ppm. However, $CH_3CO_2^-$ and HSO_4^- showed much smaller downfield shifts of about 0.04 and 0.018 ppm, respectively, which was, at most, one-third to one-fifth of that observed for $H_2PO_4^-$ and F^- (Figure 4d). 3) Although the protons showed large upfield shifts of 0.27, 0.22, and 0.12 ppm for $H_2PO_4^-$, F^- , and $CH_3CO_2^-$, respectively, the shift was almost insignificant in the presence of HSO_4^- ($\Delta\delta = 0.03$ ppm; Figure 4e). 4) The upfield shifts observed in the signal for *tert*-butyl proton s are 0.1, 0.076, 0.048, and 0.02 ppm, respectively,

for $H_2PO_4^-$, F^- , $CH_3CO_2^-$, and HSO_4^- (Figure 4f). All of these 1H NMR spectra reveal that the binding strengths of these anions follow the order $H_2PO_4^- > F^- \gg CH_3CO_2^- > HSO_4^-$; this trend is consistent with the absorption and emission results given herein. All of these results provide evidence that $H_2PO_4^-$ interacts with L_{amino} through conformational changes to the capped region, but without forming any interactions with the triazole proton or without affecting the cone conformation of the calixarene platform. On the other hand, F^- interacts with L_{amino} through the triazole moiety without resulting in significant conformational changes to the capped region or affecting the cone conformation of the calix[4]arene platform.

In the pursuit of identifying the conformational changes that occur in L_{amino} upon binding to an anion, 2D NMR spectroscopy studies were carried out (SI 10 in the Supporting Information). In the presence of $H_2PO_4^-$ or F^- , the triazole proton i loses its correlation with protons k and j. However, the cross correlation between protons a and g remains intact, which indicates that the bent conformation of the capped region persists to facilitate the interaction. Protons e and f showed interactions with a in the presence of $H_2PO_4^-$, whereas this was not present for F^- (Figure 5a). The connectivity between k and j is lost in the presence of F^- (Figure 5b). Thus, this experiment suggests that the major conformational changes observed are primarily in the capped region for $H_2PO_4^-$, whereas in the presence of F^- the triazole part of the arms is also affected.

Species detection by ESI-MS

To identify the complex(es) formed between L_{amino} and the anion, mass spectrometry studies were carried out by using $(Bu_4N)H_2PO_4$ and $(Bu_4N)F$ salts. The mass spectra showed sig-

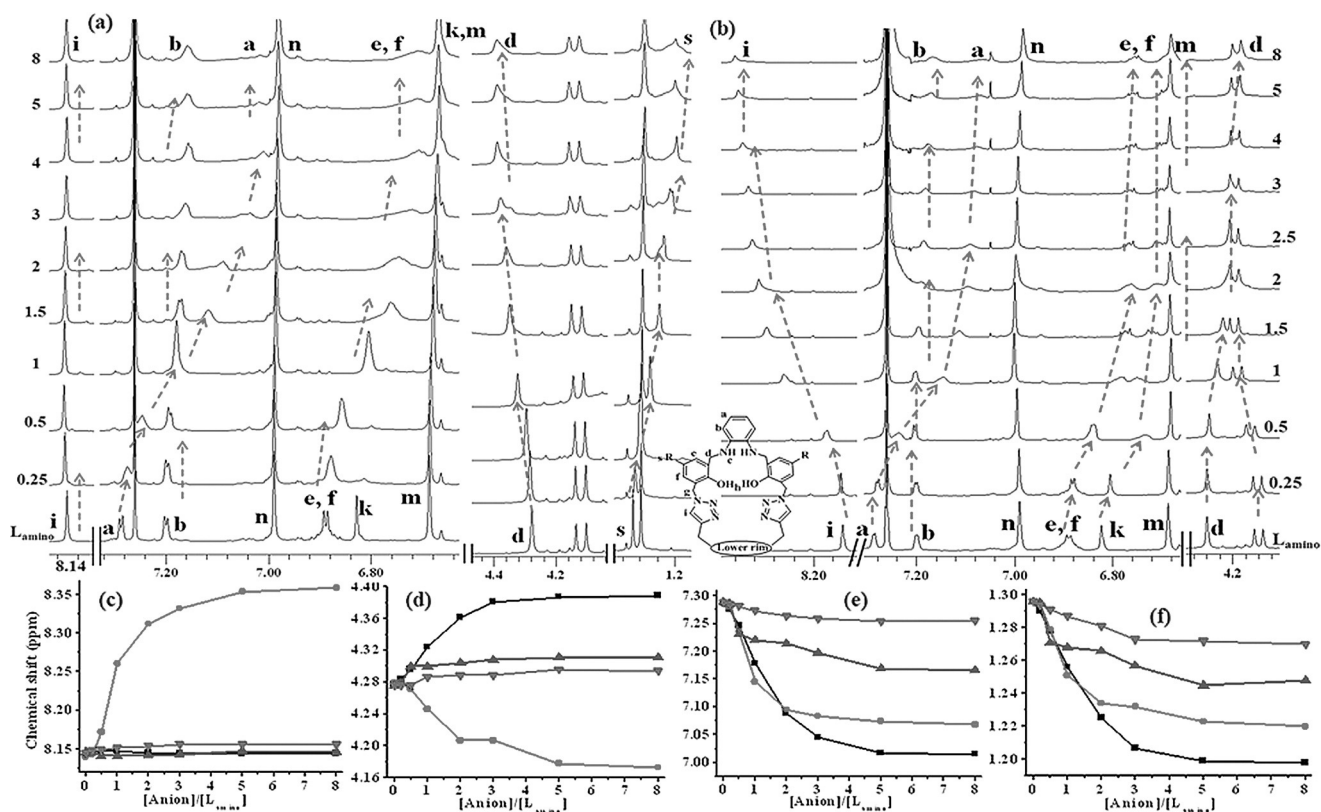


Figure 4. ¹H NMR spectroscopy titration of *L*_{aminor} with H₂PO₄⁻ (a) and F⁻ (b) in CDCl₃ at RT (the number given on the left side of each spectrum corresponds to the number of equivalents of anion added). Proton labeling is given in Scheme 1. Plots of chemical shift versus molar ratio for protons c) i, d) e, a) and f) s; ■: H₂PO₄⁻, ●: F⁻, ▲: CH₃CO₂⁻, and ▼: HSO₄⁻.

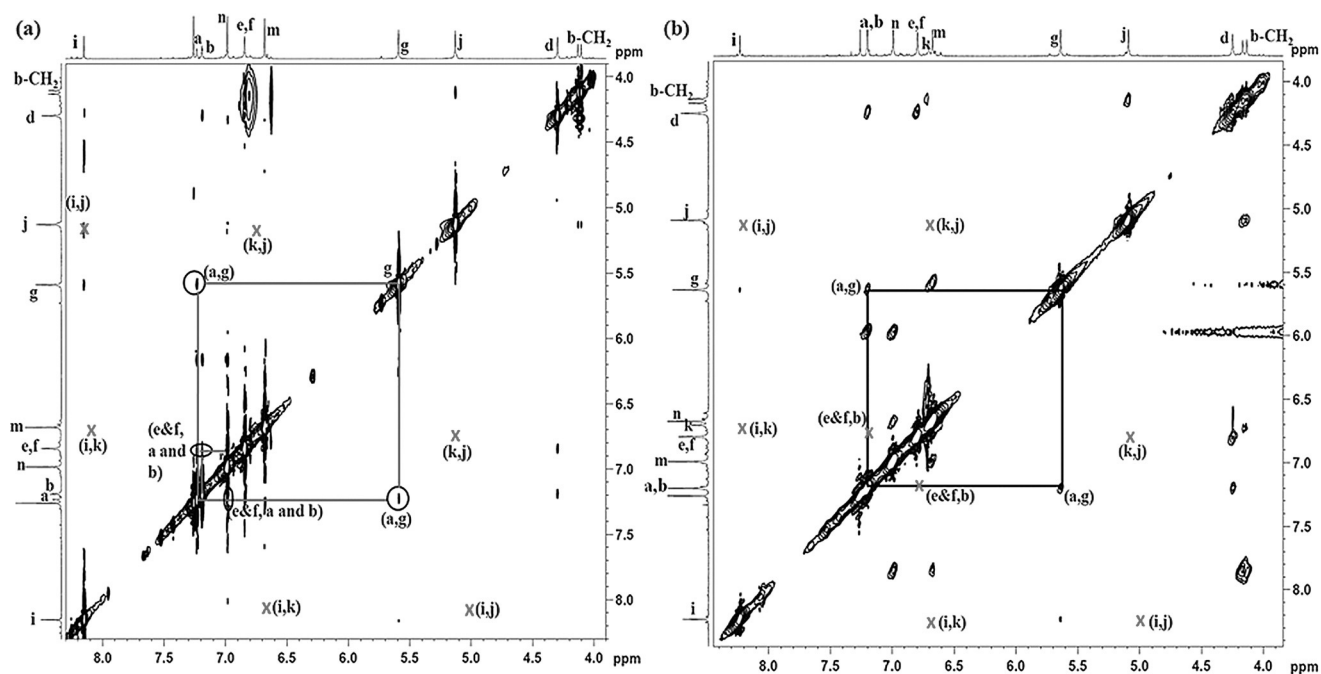


Figure 5. 2D NOESY spectra of a) *L*_{aminor} + H₂PO₄⁻ and b) *L*_{aminor} + F⁻.

nals corresponding to the anion-bound species in both cases (SI 11 in the Supporting Information). The *L*_{aminor} sample alone

shows the molecular ion signal at *m/z* 1268. When (Bu₄N)H₂PO₄ was added to *L*_{aminor}, an anion-bound species at *m/z* 1365

[$L_{\text{amino}} + \text{H}_2\text{PO}_4^-$] was observed. Even in the case of F^- , upon the addition of $(\text{Bu}_4\text{N})\text{F}$, the spectra exhibited one or more fluoride-bound species at m/z 1303 and 1327.

Requirement of the capped aminophenolic core for anion recognition

To show that the binding core formed in L_{amino} is due to capping, the control molecule, **C**, devoid of the capped aminophenolic core was studied for the absorption and emission spectra in the presence of H_2PO_4^- . No changes were found in the spectra, which supported the necessity of the capped aminophenolic binding core for the binding and recognition of H_2PO_4^- . Furthermore, the importance of the flexible $-\text{H}_2\text{C}-\text{NH}-$ core in the capped region for the recognition of H_2PO_4^- was demonstrated when the titrations were carried out with L_{imino} , which contained $-\text{HC}=\text{N}-$ instead of the amine moiety ($-\text{H}_2\text{C}-\text{NH}-$); no changes in the absorption and emission spectra were observed upon addition of H_2PO_4^- to L_{imino} (SI 12 in the Supporting Information). Thus, the capped aminophenolic core is essential for the recognition of anions.

Reversible anion sensing by L_{amino}

The fluorescence enhancement observed upon the addition of H_2PO_4^- to L_{amino} could be reversed with the addition of $\text{Mg}^{2+}/\text{Zn}^{2+}$. Therefore, the reversible sensing of L_{amino} towards H_2PO_4^- has been demonstrated when H_2PO_4^- , followed by $\text{Mg}^{2+}/\text{Zn}^{2+}$, were added consecutively for five cycles, and a reproducible fluorescence response was found for each cycle (Figure 6a and SI 13 in the Supporting Information). Thus, the addition of H_2PO_4^- to L_{amino} switches ON the fluorescence, whereas the same is switched OFF when Mg^{2+} or Zn^{2+} is added consecutively. Similar responses were observed in case of the titration of L_{amino} with F^- followed by Ca^{2+} (Figure 6b). The repeatedly demonstrated ON/OFF fluorescence behavior suggests that L_{amino} can be used as a reversible sensor for H_2PO_4^- and F^- .

Anion binding to L_{amino} measured by ITC

To understand the heat changes that occurred upon binding of H_2PO_4^- , F^- , CH_3CO_2^- , and HSO_4^- to L_{amino} , ITC studies were

performed (SI 14 in the Supporting Information). The heat changes obtained from one set of site fitting for all of these anions for this interaction followed the order $\text{H}_2\text{PO}_4^- \gg \text{F}^- > \text{CH}_3\text{CO}_2^- > \text{HSO}_4^-$ (Figure 6c and SI 14 in the Supporting Information). The data clearly show that the heat release is maximal for H_2PO_4^- , which supports the hypothesis that this anion interacts more strongly with L_{amino} than any other anion studied. Thus, this result is in accordance with that observed from spectral studies.

Supramolecular features of L_{amino} and its anion adducts

Calixarenes are known to show distinctive supramolecular features in the presence of different cations, anions, or molecules when placed on surfaces and studied by microscopy.^[58–61] The supramolecular characteristics of L_{amino} and its anion adducts were studied by SEM. The L_{amino} sample shows discrete spherical particles of 200–500 nm (Figure 7a, b, o, and p), and the features are the same, regardless of whether the molecule was taken in acetonitrile or ethanol. Even in the presence of the HSO_4^- anion, the observed SEM features are similar to that of simple L_{amino} with regard to size and shape; this suggests that no significant interactions are present between HSO_4^- and L_{amino} which alter the supramolecular characteristics (Figure 7c and d). However, in the case of CH_3CO_2^- , the L_{amino} sample reveals discrete spherical particles with a tendency to form clusters to a lesser extent, which suggests that the interaction of CH_3CO_2^- results in only minimal conformational changes to L_{amino} (Figure 7e and f). The tendency to form such aggregates, followed by their interconnection, leads to larger agglomerates and supports the formation of chainlike structures in the presence of CO_3^{2-} (Figure 7g and h). This indicates that the carbonate ion indeed interacts more strongly with L_{amino} than that of the acetate ion. When F^- (Figure 7i and j) interacts with L_{amino} , chainlike aggregation dominates and is more extensive than that observed with carbonate ions. In the presence of H_2PO_4^- , the L_{amino} sample exhibits extensively branched fibrils filled with spherical particles when taken in acetonitrile (Figure 7k and l). On the other hand, the same sample in ethanol exhibits additionally aggregated spherical particles (Figure 7m and n); thus solvent plays a role in the nature of the supramolecular structures formed.

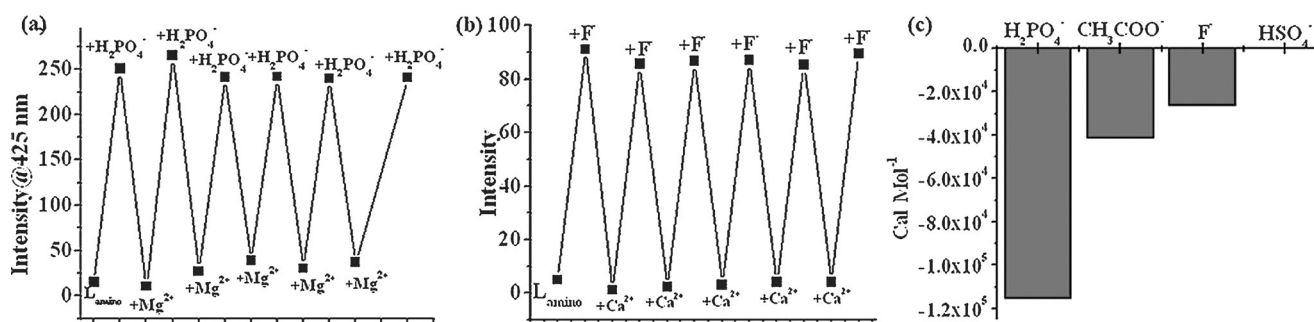


Figure 6. Reversible anion sensing detected by fluorescence spectroscopy: a) H_2PO_4^- followed by Mg^{2+} ; b) F^- followed by Ca^{2+} . c) Histogram showing the heat changes observed during the interaction of anions with L_{amino} , as monitored by ITC.

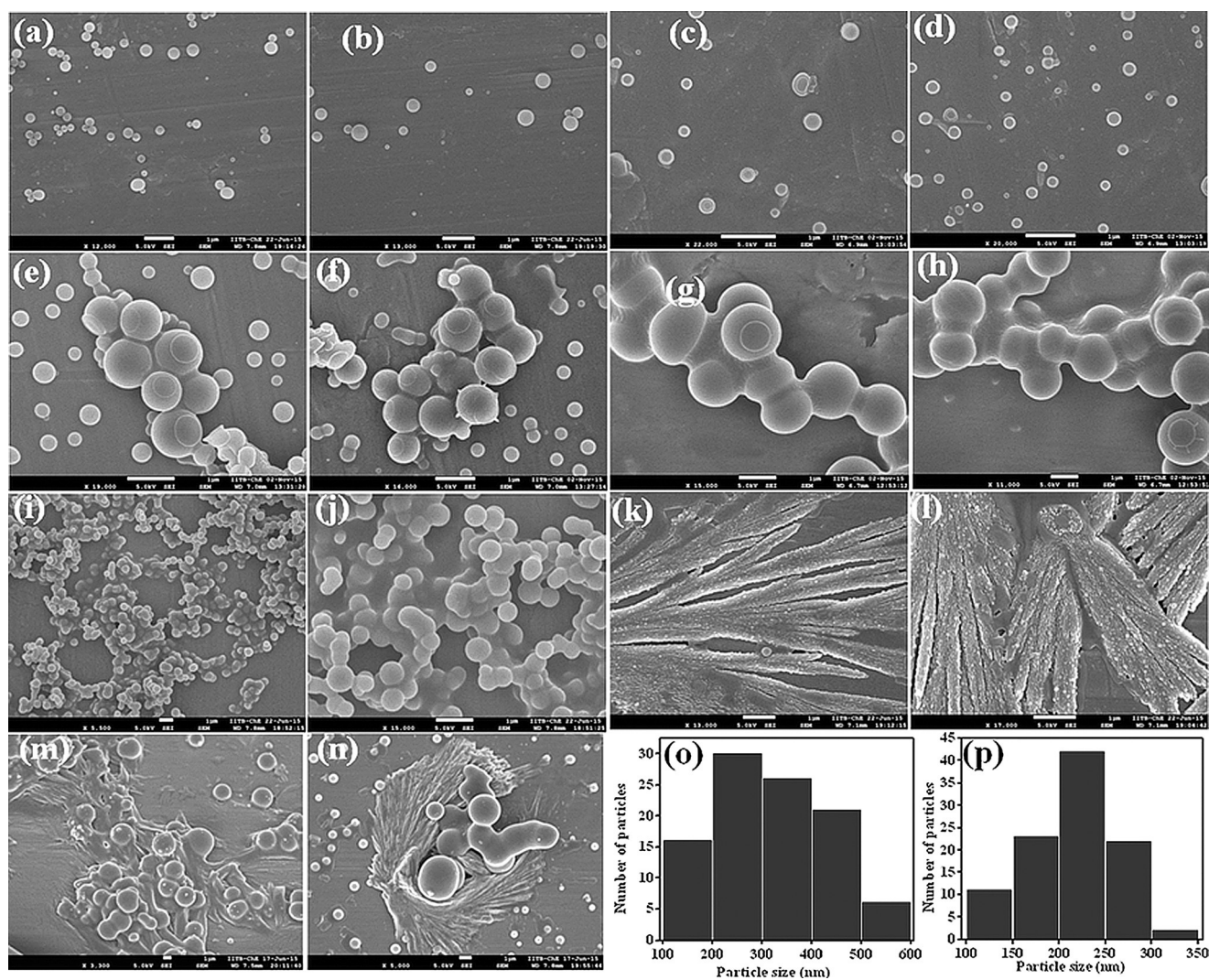


Figure 7. SEM micrographs of L_{amino} (a,b), $L_{\text{amino}} + \text{HSO}_4^-$ (c,d), $L_{\text{amino}} + \text{CH}_3\text{CO}_2^-$ (e,f), $L_{\text{amino}} + \text{CO}_3^{2-}$ (g,h), $L_{\text{amino}} + \text{F}^-$ (i,j), and $L_{\text{amino}} + \text{H}_2\text{PO}_4^-$ in acetonitrile (k,l) and ethanol (m,n). All samples were prepared in acetonitrile, unless otherwise stated. Particle size distributions for L_{amino} (o) and $\{L_{\text{amino}} + \text{HSO}_4^-\}$ (p).

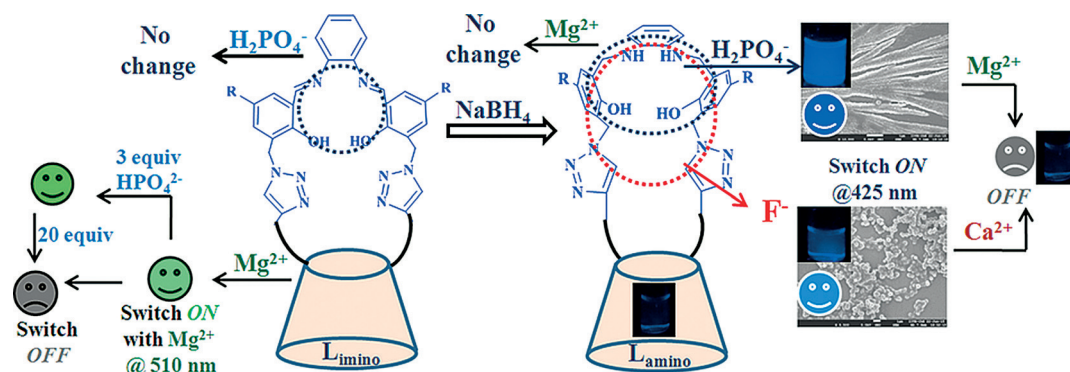
Thus, there is a smooth and sequential change in the morphological features of the particles of L_{amino} in the presence of different anions, and these changes seem to reflect the strength of their interactions with the calix conjugate upon going from acetate to carbonate to fluoride to dihydrogen phosphate, as observed by SEM. Indeed, the strength of interactions derived from spectroscopy and thermodynamics is reflected in aggregation, and the trend follows the order $\text{H}_2\text{PO}_4^- > \text{F}^- > \text{CO}_3^{2-} > \text{CH}_3\text{CO}_2^-$. This clearly demonstrates the anion-induced aggregational features of the supramolecular aspects of L_{amino} and the influence of solvent.

Conclusion

A phenylenediamine-capped conjugate of calix[4]arene (L_{amino}) was synthesized by reducing the precursor, L_{imino} , with sodium borohydride in methanol. The L_{amino} sample was recently shown by us to act as a selective receptor to Mg^{2+} cations.^[56] The anion H_2PO_4^- did not affect the spectra of the L_{imino} pre-

cursor, which suggested that L_{imino} was not a receptor for H_2PO_4^- . On the other hand, the reduced form, L_{amino} , did not show any spectral changes in the presence of cations, including Mg^{2+} (SI 15 in the Supporting Information), but was sensitive towards anions. The L_{amino} sample exhibited different interaction strengths with different anions; the most prominent were H_2PO_4^- and F^- . These two ions are differentiated not only based on their spectra, but also on the supramolecular features revealed by SEM. Thus, these two conjugates, L_{imino} and L_{amino} , exhibit complementarity in their sensing behavior towards ions (Scheme 2).

The L_{amino} sample showed good selectivity towards H_2PO_4^- over 15 anions studied, including other phosphates, such as $\text{P}_2\text{O}_7^{4-}$, AMP^{2-} , ADP^{2-} , and ATP^{2-} . The absorption studies of L_{amino} with anions revealed that H_2PO_4^- , CO_3^{2-} , HCO_3^- , CH_3CO_2^- , and F^- showed an increase in the absorbance at $\lambda = 315$ nm among the phosphates, halides, and oxoanions (HSO_4^- , NO_3^- , SO_4^{2-} , and ClO_4^-) studied. Upon the interaction of L_{amino} with H_2PO_4^- , the emission band at $\lambda = 425$ nm



Scheme 2. Schematic representation of the complementarity of the sensing behavior of L_{imino} versus L_{amino} .

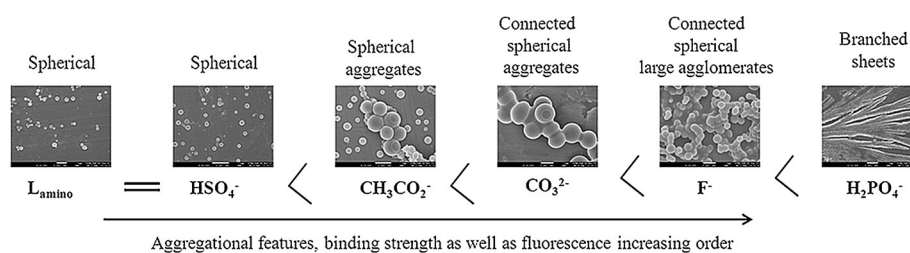


Figure 8. Relationship between binding strength and aggregation.

showed an enhancement of about 21-fold, whereas the ratiometric enhancement (I_{425}/I_{315}) was about ≈ 11 -fold; thus, an increase in the quantum yield by an order of magnitude in presence of H_2PO_4^- was observed. The present study, including ESI-MS experiments, supported the formation of a 1:1 complex with $K_a = 6.18 \times 10^4 \text{ M}^{-1}$ and provided a minimum detection limit of $(1.2 \pm 0.2) \mu\text{M}$ ($(116 \pm 20) \text{ ppb}$) for H_2PO_4^- with L_{amino} . Even other anions, such as F^- , CO_3^{2-} , HCO_3^- , and CH_3CO_2^- , also exhibited a ratiometric increase, but to a much lesser extent.

^1H NMR spectroscopy titration of L_{amino} with H_2PO_4^- revealed that the interaction led to changes in chemical shift mainly in the capped region, and thus, provided evidence of the aminophenolic region as the binding core for H_2PO_4^- . However, other anions, such as F^- , CH_3CO_2^- , and HSO_4^- , exhibited much smaller changes in chemical shifts of the protons present in the binding region, which suggested that the binding strength of these anions followed the order $\text{H}_2\text{PO}_4^- > \text{F}^- \gg \text{CH}_3\text{CO}_2^- > \text{HSO}_4^-$. This trend is the same for the absorption and emission data. The conformational changes induced in L_{amino} upon interaction with anion were detected by NOESY experiments, and the data supported changes to the capped region upon binding H_2PO_4^- ; this also extended to the triazole part for F^- . The L_{amino} sample exhibited a reversible ON/OFF response in the presence of H_2PO_4^- followed by Mg^{2+} for five cycles, and similar results were obtained for the addition of F^- followed by Ca^{2+} . The ITC experiments provided evidence that the changes in heat observed upon interaction with an anion followed a trend that paralleled the binding strengths monitored from the chemical shifts observed in the spectra. In SEM micrographs of L_{amino} , spherical particles are transformed into spheri-

cal aggregates, large agglomerates, and finally to branched sheets in the presence of the anions, depending upon the binding strength (Figure 8).

Thus, although L_{imino} is sensitive to cations, in particular, to Mg^{2+} , the L_{amino} sample, obtained from the reduction of the imino-capped derivative to its amino form, is sensitive to anions, in particular, to H_2PO_4^- . The conformational flexibility of L_{amino} , particularly in the capped region, is responsible for this transformation in the sensing behavior observed. Indeed, this was reflected in features observed by both spectroscopy and microscopy.

Acknowledgements

C.P.R. acknowledges financial support from the DST (SERB and Nano mission), CSIR, and DAE-BRNS. C.P.R. acknowledges the DST (SERB) for a J. C. Bose National Fellowship and IIT Bombay for an Institute Chair Professorship. Fellowships from UGC for A.N. and D.S.Y. are gratefully acknowledged. We thank the FEGSEM central facility of IIT Bombay for providing the service.

Keywords: anions · calixarenes · sensors · structure–activity relationships · supramolecular chemistry

- [1] P. D. Beer, *Chem. Commun.* **1996**, 689.
- [2] F. P. Schmidtchen, M. Berger, *Chem. Rev.* **1997**, 97, 1609.
- [3] P. D. Beer, P. A. Gale, *Angew. Chem. Int. Ed.* **2001**, 40, 486; *Angew. Chem.* **2001**, 113, 502.
- [4] G. Liu, J. Shao, *J. Inclusion Phenom. Macrocyclic Chem.* **2013**, 76, 99.
- [5] J. R. Hiscock, P. A. Gale, M. J. Hynes, *Supramol. Chem.* **2012**, 24, 355.
- [6] P. A. Gale, S. E. G. Garrido, J. Garric, *Chem. Soc. Rev.* **2008**, 37, 151.

- [7] M. D. Best, S. L. Tobey, E. V. Anslyn, *Coord. Chem. Rev.* **2003**, *240*, 3.
- [8] F. P. Schmidtchen, *Coord. Chem. Rev.* **2006**, *250*, 2918.
- [9] R. Matínez-Máñez, F. Sancenón, *Chem. Rev.* **2003**, *103*, 4419.
- [10] C. Suksai, T. Tuntulani, *Chem. Soc. Rev.* **2003**, *32*, 192.
- [11] S. L. Wiskur, H. Ait-Haddou, J. J. Lavigne, E. V. Anslyn, *Acc. Chem. Res.* **2001**, *34*, 963.
- [12] P. A. Gale, *Coord. Chem. Rev.* **2001**, *213*, 79.
- [13] T. S. Snowden, E. V. Anslyn, *Curr. Opin. Chem. Biol.* **1999**, *3*, 740.
- [14] J. L. Sessler, J. M. Davis, *Acc. Chem. Res.* **2001**, *34*, 989.
- [15] E. A. Katayev, Y. A. Ustynuk, J. L. Sessler, *Coord. Chem. Rev.* **2006**, *250*, 3004.
- [16] C. B. Black, B. Andrioletti, A. C. Try, C. Ruiperez, J. L. Sessler, *J. Am. Chem. Soc.* **1999**, *121*, 10438.
- [17] J. L. Sessler, D. G. Cho, V. Lynch, *J. Am. Chem. Soc.* **2006**, *128*, 16518.
- [18] V. Kral, O. Rusin, T. Shishkanova, R. Volf, P. Matejka, K. Volka, *Chem. Listy* **1999**, *63*, 546.
- [19] S. Licen, V. Bagnacani, L. Baldini, A. Casnati, F. Sansone, M. Giannetto, P. Pengo, P. Tecilla, *Supramol. Chem.* **2013**, *25*, 631.
- [20] N. Y. Edwards, F. Liu, G. Chen, *Supramol. Chem.* **2013**, *25*, 481.
- [21] P. Thuéry, B. Masci, *Cryst. Growth Des.* **2010**, *10*, 716.
- [22] P. Thuéry, *Cryst. Growth Des.* **2011**, *11*, 2606.
- [23] R. Joseph, C. P. Rao, *Chem. Rev.* **2011**, *111*, 4658.
- [24] V. V. S. Mummdivarapu, D. S. Yarramala, K. K. Kondaveeti, C. P. Rao, *J. Org. Chem.* **2014**, *79*, 10477.
- [25] M. Kandpal, A. K. Bandela, V. K. Hinge, V. R. Rao, C. P. Rao, *ACS Appl. Mater. Interfaces* **2013**, *5*, 13448.
- [26] V. V. S. Mummdivarapu, A. Nehra, V. K. Hinge, C. P. Rao, *Org. Lett.* **2012**, *14*, 2968.
- [27] S. E. Matthews, P. D. Beer, *Supramol. Chem.* **2005**, *17*, 411.
- [28] B. Tomapatanaget, T. Tuntulani, *Tetrahedron Lett.* **2001**, *42*, 8105.
- [29] B. Tomapatanaget, T. Tuntulani, O. Chailapakul, *Org. Lett.* **2003**, *5*, 1539.
- [30] Y. Takeuchi, T. Sakurai, K. Tanaka, *Main Group Met. Chem.* **2000**, *23*, 311.
- [31] V. V. S. Mummdivarapu, R. K. Pathak, V. K. Hinge, J. Dessingou, C. P. Rao, *Supramol. Chem.* **2014**, *26*, 538.
- [32] R. K. Pathak, K. Tabbasum, A. Rai, D. Panda, C. P. Rao, *Anal. Chem.* **2012**, *84*, 5117.
- [33] T. Gunnlaugsson, M. Glynn, G. M. Tocci, P. E. Kruger, F. M. Pfeffer, *Coord. Chem. Rev.* **2006**, *250*, 3094.
- [34] E. M. Nolan, S. J. Lippard, *Chem. Rev.* **2008**, *108*, 3443.
- [35] Y. Yang, Q. Zhao, W. Feng, F. Li, *Chem. Rev.* **2013**, *113*, 192.
- [36] J. Fan, M. Hu, P. Zhan, X. Peng, *Chem. Soc. Rev.* **2013**, *42*, 29.
- [37] W. Saenger, *Principles of Nucleic Acid Structure*, Springer, New York, **1988**.
- [38] A. P. de Silva, H. Q. N. Gunaratne, T. Gunnlaugsson, A. J. M. Huxley, C. P. McCoy, J. T. Rademacher, T. E. Rice, *Chem. Rev.* **1997**, *97*, 1515.
- [39] J. P. Desvergue, A. W. Czarnik, *Chemosensors for Ion and Molecular Recognition*, Kluwer Academic Publishers, Dordrecht, **1997**.
- [40] W. Gong, K. Hiratani, *Tetrahedron Lett.* **2008**, *49*, 5655.
- [41] S. I. Kondo, Y. Hiraoka, N. Kurumatani, Y. Yano, *Chem. Commun.* **2005**, 1720.
- [42] G.-D. Shun, Z.-P. Liu, J.-P. Ma, R.-Q. Huang, *Tetrahedron Lett.* **2007**, *48*, 1221.
- [43] H. Ihm, S. Yun, H. G. Kim, J. K. Kim, K. S. Kim, *Org. Lett.* **2002**, *4*, 2897.
- [44] K. Choi, A. D. Hamilton, *Angew. Chem. Int. Ed.* **2001**, *40*, 3912; *Angew. Chem.* **2001**, *113*, 4030.
- [45] T. H. Kwon, K. S. Jeong, *Tetrahedron Lett.* **2006**, *47*, 8539.
- [46] Z. Xu, S. Kim, K. H. Lee, J. Yoon, *Tetrahedron Lett.* **2007**, *48*, 3797.
- [47] S. Sasaki, D. Citterio, S. Ozawa, K. Suzuki, *J. Chem. Soc. Perkin Trans. 2* **2001**, 2309.
- [48] H. Xie, S. Yi, X. Yang, S. Wu, *New J. Chem.* **1999**, *23*, 1105.
- [49] K. Ghosh, A. R. Sarkar, A. P. Chattopadhyay, *Eur. J. Org. Chem.* **2012**, 1311.
- [50] P. Plitt, D. E. Gross, V. M. Lynch, J. L. Sessler, *Chem. Eur. J.* **2007**, *13*, 1374.
- [51] C. Y. Chang, L. X. Xian, H. Hong, W. W. Wei, Z. Y. Song, *Sci. China Chem.* **2010**, *53*, 569.
- [52] S. H. Kim, I. J. Hwang, S. Y. Gwon, S. M. Burkinshaw, Y. A. Son, *Dyes Pigm.* **2011**, *88*, 84.
- [53] J. S. Bae, S. Y. Gwon, S. Matsumoto, Y. A. Son, S. H. Kim, *Fibers Polym.* **2009**, *10*, 858.
- [54] V. V. S. Mummdivarapu, V. K. Hinge, K. Tabbasum, R. G. Gonnade, C. P. Rao, *J. Org. Chem.* **2013**, *78*, 3570.
- [55] V. V. S. Mummdivarapu, V. K. Hinge, K. Samanta, D. S. Yarramala, C. P. Rao, *Chem. Eur. J.* **2014**, *20*, 14378.
- [56] A. Nehra, V. K. Hinge, C. P. Rao, *J. Org. Chem.* **2014**, *79*, 5763.
- [57] A. Hens, K. K. Rajak, *RSC Adv.* **2015**, *5*, 44764.
- [58] A. Nehra, D. S. Yarramala, V. K. Hinge, K. Samanta, C. P. Rao, *Anal. Chem.* **2015**, *87*, 9344.
- [59] V. V. S. Mummdivarapu, K. Tabbasum, J. P. Chinta, C. P. Rao, *Dalton Trans.* **2012**, *41*, 1671.
- [60] R. Joseph, B. Ramanujam, A. Acharya, A. Khutia, C. P. Rao, *J. Org. Chem.* **2008**, *73*, 5745.
- [61] J. Dessingou, A. Mitra, K. Tabbasum, G. S. Baghel, C. P. Rao, *J. Org. Chem.* **2012**, *77*, 371.

Received: February 9, 2016
Published online on May 24, 2016